Performance of Sub-Nyquist Sampling Based on The MWC System for 5G Mobile Communication Networks

Fatemeh Ghorbaniparvar[1,*], Gerald Arada[2], Lawrence Materum[2]

1   Department of Aeronatical, Automotive and Offfshore Engineering, Fakulti Kejuruteraan Mekanikal, Universiti Teknologi Malaysia, 81310 Skudai, Johor, Malaysia
2   Department of Mechanical Engineering, Faculty of Engineering, Kano University of Science and Technology, Wudil, Nigeria

ARTICLE INFO	ABSTRACT
Keywords: Multichannel sampling; 5G networks; Sub-Nyquist; MWC; Multiband signals	The fifth-generation (5G) mobile network has been positioned to be a critical part of wireless communication networks. Decreasing receiver complexity and reducing power consumption are essential 5G communication systems design targets. One approach for achieving these goals is to employ sampling methods at sub-Nyquist rates that reduce the burden on hardware devices while enabling accurate reconstruction. Modulated Wideband Converter (MWC) is a system that uses a multichannel sampling method at a low sub-Nyquist rate, which leads to simple hardware. This paper investigates the application of multichannel sub-Nyquist sampling to high-frequency multiband signals in a 5G network. We sample and reconstruct multiband signals using the method based on MWC technology utilizing the concept of compressed sensing, which can prevent the difficulties of signal sampling caused by wide bandwidth and high frequencies. The signal is mixed with a pseudorandom sign waveform in each channel during the sampling stage. A lowpass filter filters the mixed signal before applying a low sampling rate. For the reconstruction of the signal, the system estimates spectrum support and then reconstructs the active bands of the signal. The experimental results indicate that the MWC system is an effective sampling method for multiband signals in both frequency ranges, sub-6 GHz frequencies and millimeter-wave frequencies, in 5G mobile communication networks, and its reconstruction performance is acceptable.

1. Introduction

Fifth-generation mobile communication networks operate across a broad range of frequencies, utilizing both sub-6 GHz frequencies that are lower than 6 GHz, and millimeter-wave (mm-wave) frequencies that range from 24 to 100 GHz and provide extremely high data rates [1]. Fifth-generation wireless networks employ higher carrier frequencies to support rising peak data rates and area capacity [1-2]. There are growing demands for mm-wave technologies. There have been substantial improvements in millimeter-wave (mm-wave) technologies. These growths are due to their attractive properties, which make them useful in a variety of practical applications [23].

---

* Corresponding author.
E-mail address: fatemeh_ghorbaniparvar@dlsu.edu.ph

Millimeter-wave (mm-wave) communications are indeed a crucial component of 5G mobile communication networks [3-4]. The use of millimeter-wave communications is expected to present additional challenges. Many nations have opened to the 60 GHz millimeter-wave frequency band, including South Korea, Japan, and the United States, because the area around 60 GHz has an abundance of usable spectrum to allow high-rate wireless communications [5].

When developing sampling methods, periodic nonuniform sampling is considered [6]. Uniform sampling is a strategy where samples are dispersed equally across time, with no significant reduction in the sampling rate. Because they cannot reduce rates more than Nyquist approaches, nonuniform sampling methods are more frequently used [7-8]. One technique for nonuniform sampling is random sampling [9]. If the original signal is sparse in the frequency domain, it can be very accurately reconstructed from the signal recorded using random sampling [9]. There is a close relationship between compressive sensing and this random sampling feature [10]. Novel ideas for multiband signal processing [11-12] were introduced by the quick development of compressed sensing (CS) theory, which helped address the issues of big data and large bandwidths. Furthermore, demodulation, which lowers the sampling rate below the Nyquist rate, is the most widely utilized sub-Nyquist sampling method for multiband signals [13]. The MWC is a system that employs the idea of the random demodulator [12] to sample a signal at a compressed rate, namely, far beneath the Nyquist rate, and then uses compressed sensing algorithms to reconstruct the signal [14].

The Internet has become a vital global connection tool that people use every day through different devices like phones, computers, and smart TVs for different activities such as online shopping, and online meetings. This results in an increased demand for faster speeds and the need for higher transmission capacities [24]. In contrast to 4G and previous generations, 5G will alter the physical layer, which will impact the receiver's needs. It must receive a high-frequency signal to reassemble the transmitted data [15]. The transmission signal will transform into a wideband signal to transmit data faster. As a result, it will put additional strain on storage and sampling devices, especially regarding hardware implementation. Consequently, the wideband multiband signal sampled at the sub-Nyquist rate is receiving increasing attention. Due to its ability to process broadband signals, the modulated wideband converter system appears to be the best choice for processing multiband signals with sparse spectrum structures. For millimeter-wave systems, it can circumvent the difficulties in signal sampling that arise at high frequencies and large bandwidths [16].

Wideband spectrum sensing has been accomplished in the field of cognitive radio through the widespread use of the MWC system [17-18]. While the MWC technique uses compressed sensing to reconstruct signals [14], several drawbacks degrade the reconstruction performance and prevent it from operating at optimal levels. Current studies cannot provide a clear solution, which causes the signal reconstruction to function inconsistently and unacceptably. The millimeter wavelength spectrum has recently garnered attention in the wireless communication world. Utilizing the vast, unused bandwidth to support upcoming multi-gigabit-per-second mobile, imaging, and multimedia applications is the concept underlying millimeter-wave communications [3]. However, there have been efforts to enhance mobile network performance, but there is still an important gap between the capabilities promised by the networks and the users' experiences, and it causes an increasing demand for fast internet [22]. Regarding improved quality and higher data rates for internal users, millimeter-wave communication technologies offer a bright future [2]. For attaining a greater transmission rate, the transmission signal is transformed into a broadband signal. Thus, sampling and storage devices will be under increased pressure, particularly regarding hardware implementation. This outcome leads to more attention being paid to the broadband multiband signal sampled at the sub-Nyquist rate. Because of its capacity to process broadband signals, the MWC system appears to be the optimal option for processing multiband signals with sparse spectrum structures. The MWC

method lessens the strain on storage devices. It lowers the hardware complexity brought on by the high frequencies and large bandwidth of 5G network transmissions by using spectrum aliasing to obtain a low sub-Nyquist rate for signal sampling. This paper elucidates that the MWC technology can sample multiband signals in both frequency ranges (mm-wave frequencies and sub-6 GHz frequencies) in 5G mobile networks at rates far below the Nyquist rate, and then reconstruct them successfully.

2. The Modulated Wideband Converter System

Because high rates of sampling in Nyquist systems present challenges, sub-Nyquist methods are receiving more attention from academic and industrial sectors. The sub-Nyquist system, known as the MWC, is a system that has made it possible for multiband signals to be sampled at low sub-Nyquist rates. MWC consists of two parts: the sampling and the reconstruction. For sampling the signal, the input signal simultaneously enters multiple channels. Next, a periodic function is multiplied by the signal in each channel. The idea behind the mixing stage is to disperse the spectrum in a way that a piece of energy of each band emerges in the baseband. Following the mixing stage, a lowpass filter is used to filter the signal spectrum before it is sampled at a low rate that corresponds to the lowpass cutoff. For reconstruction of the signal, the system estimates spectrum support. After determining the unknown spectrum support, digital processing is used to reconstruct the input signal's active bands [14].

2.1 The Sampling Method

The signal $x(t)$ simultaneously enters m channels during the sampling phase. In the ith channel, $x(t)$ is subsequently multiplied by a periodic waveform, $p_i(t)$. The piecewise constant function $p_i(t)$ has a period of T_p and alternates between +1 and -1 [20]. After the multiplication step, it is filtered using a lowpass filter with a cut-off frequency of $1/(2T_s)$, then the output is uniformly sampled at a rate of $1/T_s$. The sampling interval T_s is equal to T_p (the period of $p_i(t)$). The sampling part of the MWC system is illustrated in Figure 1.
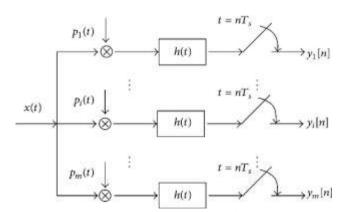

Fig. 1. The sampling part of MWC

The total sampling frequency of the MWC is $m(1/T_s)$. It is assumed that the input $x(t)$ is a wideband signal with a Nyquist frequency (f_{nyq}), which can be significantly bigger than the sampling frequency m/T_s. The support of $x(t)$ resides within N bands and the width of each band does not go beyond B Hz. The band locations are arbitrary and particularly unidentified beforehand.

Baseband frequencies that are below the cut-off frequency of the filter have a combination of the spectral components from the whole Nyquist range due to the alteration of the spectrum of $x(t)$ caused by the mixing process. By mixing the signal with the periodic function $p_i(t)$, the spectrum is spread so that a part of each band's energy is visible in the baseband. This is the crucial phase that makes the MWC capable of sub-Nyquist rate signal sampling. For instance, imagine a single channel, and let $P_i(f)$ be the spectrum of $p_i(t)$ (the mixing function). Because $p_i(t)$ is T_p - periodic, $P_i(f)$ can be stated as:

$$P_i(f) = \sum_{l=-\infty}^{\infty} c_{il}\delta(f - lf_P) \tag{1}$$

where $f_P = 1/T_p$, c_{il} are arbitrary coefficients, and $\delta()$ is the Dirac delta function. In this way, the spectrum of the mixed signal $\tilde{x}_i(t) = x(t)p_i(t)$ is:

$$\tilde{X}_i(f) = P_i(f) * X(f) = \sum_{l=-\infty}^{\infty} c_{il}X(f - lf_P). \tag{2}$$

$X(f)$ is the spectrum of $x(t)$. After lowpass filtering with a filter function $H(f)$, the result will be a signal $y_i(t)$ with a spectrum as below:

$$Y_i(f) = \sum_{l=-\infty}^{\infty} c_{il}X(f - lf_P)H(f). \tag{3}$$

We sample the signal $y_i(t)$ at rate $f_s = 1/T_s$, then take the discrete-time Fourier transform (DTFT) of the samples $y_i[n]$ as:

$$Y_i(e^{j\omega}) = \sum_{k=-\infty}^{\infty} Y\left(\frac{f_s}{2\pi}(w - 2k\pi)\right) = \sum_{l,k=-\infty}^{\infty} c_{il}X\left(\frac{f_s}{2\pi}w - lf_P - kf_s\right)H(\frac{f_s}{2\pi}w - kf_s) \tag{4}$$

for $\omega \in [-\pi, \pi]$. In the standard modulated wideband converter, $H(f)$ is considered an ideal $rect$ function with a cutoff $f_s/2$. Therefore, $H(\frac{f_s}{2\pi}w - kf_s)$, $\omega \in [-\pi, \pi]$, is nonzero only if $k = 0$. To ease the explanation, we select $T_s = T_p$. Then, Eq. (4) can be rewritten as:

$$Y_i(e^{j\omega}) = \sum_{l=-L_0}^{L_0} c_{il}X\left(\frac{f_p}{2\pi}w - lf_P\right) \qquad \omega \in [-\pi, \pi] \tag{5}$$

L_0 is the smallest integer satisfying $2L_0 + 1 > f_{nyq}/f_P$. It's more practical to write down Eq. (5) in matrix form as stated below:

$$y(e^{j\omega}) = Az(\omega) \tag{6}$$

$y(e^{j\omega})$ is an $m \times 1$ vector with the ith element $Y_i(e^{j\omega})$, $z(\omega)$ is an unknown vector of length $L = 1 + 2L_0$ with the ith element $z_i(\omega) = X\left(\frac{f_p}{2\pi}w - (i - L_0 - 1)f_P\right)$. Also, A is an $m \times L$ matrix holding the coefficients c_{il}. It can be seen that $X\left(\frac{f_p}{2\pi}w - lf_P\right)$, for $|l| \le L_0$, contains all the spectral information of $x(t)$. Hence, to regain $x(t)$, it is enough to establish $z(\omega)$ for every $\omega \in [-\pi, \pi]$.

Because of the sparse nature of the spectrum of $x(t)$, the vector $z(\omega)$ is sparse for each $\omega \in [-\pi, \pi]$. The sparsity of $z(\omega)$ makes MWC able to recover $x(t)$ with a few channels, which means sub-Nyquist sampling.

2.2 Reconstruction Method

In the reconstruction part that is fully executed in the time domain, the spectral support is initially established. The signal is then reconstructed from the samples.

The process of spectral support recovery is based on ideas developed in compressed sensing [19]. It involves a series of digital calculations grouped under the Continuous-to-Finite (CTF) block [20–21]. In order to recover the support of active bands, we utilize the CTF block. We can reconstruct each signal band using a direct pseudoinverse operation once the support is provided. The signal bands are then modulated to their related carrier frequencies. Consider the support of $z(\omega)$ to be $S = \bigcup_{w \in [-\pi,\pi]} \text{supp}(z(\omega))$, where supp() is the set of indices of the nonzero entries of a vector. It means if $i \notin S$ then $z_i(\omega) = 0$ for all $\omega \in [-\pi, \pi]$. By using the sparsity of $z(\omega)$, the CTF effectively infers the support S from a low-complexity finite program.

When the support S is concluded, it follows from Eq. (6) that:

$$z_S[n] = A_S^{\dagger} y[n], \qquad\qquad\qquad z_i[n] = 0, \quad i \notin S \qquad\qquad (7)$$

where $z[n] = (z_1[n], \dots, z_L[n])^T$ and $z_i[n]$ is the inverse discrete-time Fourier transform of $z_i(\omega)$. $z_S[n]$ and A_S mean the subvector and submatrix comprised of the rows of $z[n]$ and A indexed by S, in turn. The notation () † states the pseudoinverse. Eq. (7) permits $z_i[n]$ to be made at the input rate f_s. Then, every $z_i[n]$ is interpolated to a baseband signal at the rate f_s yielding $z_i(t)$:

$$z_i(t) = \sum_{n=-\infty}^{\infty} Z_i[n]h(t - nT_s), \qquad\qquad\qquad\qquad (8)$$

where $h(t) = \text{sinc}(\pi t/T_s)$. In the end, modulating $z_i(t)$ to the appropriate bands reconstructs $x(t)$:

$$\hat{x}(t) = \sum_{i \in S, i > L_0} \text{Re}\{z_i(t)\}\cos(2\pi i f_P t) + \text{Im}\{z_i(t)\}\sin(2\pi i f_P t) \qquad\qquad (9)$$

The real and imaginary parts of their argument are denoted by Re() and Im().

3. Simulation Results

To assess the MWC system's effectiveness for multiband signals in 5G mobile communication networks, we perform the simulations. We consider a model, as explained below, for a multiband signal in 5G mobile communication networks.

$$x(t) = \sum_{i=1}^{N/2} \sqrt{E_i B} \ \text{sinc}(B(t - \tau_i)) \cos(2\pi f_i(t - \tau_i)). \qquad\qquad (10)$$

The signal model describes a multiband signal with N bands that are symmetrical pairs. Each band is of width B, and E_i represents the energy of each pair of bands. The time offsets shown by τ_i and the carrier frequencies f_i for each pair of bands are chosen to be smaller than $f_{\text{nyq}}/2$ [14], [20] at random in the desired range in 5G networks. In addition, we generate white Gaussian noise so that its spectrum is in $[-f_{\text{nyq}}/2, f_{\text{nyq}}/2]$, and add it to the input signal. We assess the system's performance in two ranges of frequencies (sub-6 GHz and mm-wave) by altering the carrier frequency and the bandwidth of the signal model. Parameters of τ_i, Ei, N, M remain unchanged during the evaluation process. M is a parameter in the MWC system that presents the compression ratio, and its value in this paper is considered 195 [14].

First, we investigate the performance of the system by changing the carrier frequency f_i which is selected at random in the range of sub-6 GHz frequencies in 5G networks [1] as shown in Table 1. The values of B and N are considered as 45 MHz and 2, respectively. The sampling frequency of each channel f_s is equal to f_{nyq}/M, and the total sampling rate is equal to $f_s \times$ channel number [14], [20]. As Table 1 depicts, the reconstruction performance of the system is not successful for f_i = 2 GHz, but when f_{nyq} is 8 GHz, MWC can reconstruct the input successfully. For the other two randomly chosen carrier frequencies, the MWC can sample the signal far below the Nyquist rate and then reconstruct them successfully.

Table 1
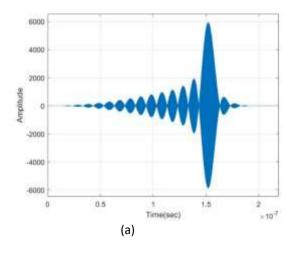Performance of MWC for different sub-6 GHz carrier frequencies

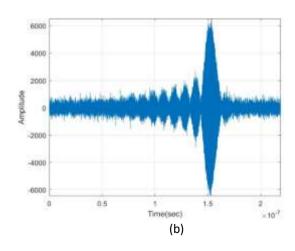| f_i	f_{nyq}	Total sampling rate	Number of channels	Reconstruction
2 GHz	5 GHz	769,230,770 Hz	30	Unsuccessful
1.55 GHz	5 GHz	769,230,770 Hz	30	Successful
2 GHz	8 GHz	1,230,769,231 Hz	30	Successful
3 GHz	8 GHz	1,230,769,231 Hz	30	Successful

In Table 2, we select the f_i in the range [30 GHz, 60 GHz] (millimeter-wave frequencies) randomly and put the values of B and N at 100 MHz and 2, respectively. It shows that the MWC can reconstruct three signals out of the four randomly chosen signals successfully with a sampling rate far below the Nyquist rate.
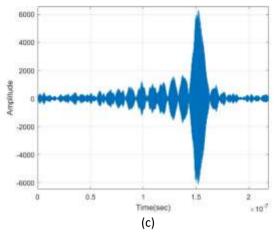
Table 2
Performance of MWC for different millimeter-wave carrier frequencies

f_i	f_{nyq}	Total sampling rate	Number of channels	Reconstruction
30 GHz	70 GHz	10,769,230,770 Hz	30	Successful
40 GHz	90 GHz	13,846,153,847 Hz	30	Successful
60 GHz	130 GHz	20,000,000,000 Hz	30	Successful
60 GHz	120 GHz	18,461,538,461 Hz	30	Unsuccessful

As Figure 2 shows, the MWC can reconstruct the input signal successfully despite the presence of noise. In this case, the sampling rate of the system is approximately six times lower than the Nyquist rate.
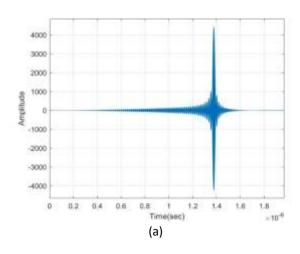

(a)

(b)

(c)

Fig. 2. Reconstruction performance of the MWC (a) The original signal (b) The signal with the presence of noise (c) Reconstructed signal, when f_i and f_{nyq} are 40 GHz and 90 GHz, respectively.
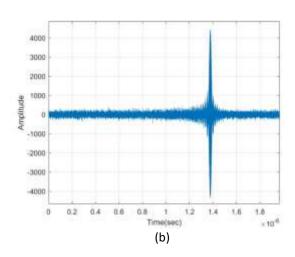
Table 3 shows the results of our evaluation of MWC's performance in 5G networks when we vary the bandwidth in the sub-6 GHz frequency range. The f_i and f_{nyq} are chosen randomly as 2 GHz and 10 GHz, while N is considered at 2. Sampling frequencies (f_s) for each channel is f_{nyq}/M (10GHz/195) for the four bandwidths shown in Table 3. So, the total sampling rate for 30 channels is 30×(10GHz/195). As we can see in Table 3, with the same sample rate, the reconstruction performance of the signal is successful for bandwidths of 20 MHz and 50 MHz and is unsuccessful for bandwidths of 60 MHz and 80 MHz due to the system's inability to establish the spectral support.
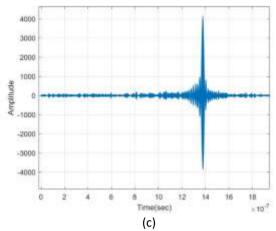
Table 3
Performance of MWC for different bandwidths at sub-6 GHz carrier frequency range

Bandwidth	Total sampling rate	Number of channels	Reconstruction
20 MHz	1,538,461,539 Hz	30	Successful
50 MHz	1,538,461,539 Hz	30	Successful
60 MHz	1,538,461,539 Hz	30	Unsuccessful
80 MHz	1,538,461,539 Hz	30	Unsuccessful

The original signal, the signal with noise, and the reconstructed signal are shown in Figure 3 when N and B are 2 and 60 MHz, respectively.

(a)

(b)

7

(c)

Fig. 3. Reconstruction performance of the MWC (a) The original signal (b) The signal with the presence of noise (c) reconstructed signal, when f_i and f_{nyq} are 2 GHz and 10 GHz, respectively.

Table 4 shows the results of our evaluation of MWC's performance with various bandwidth values. But, in this step, f_i is chosen from the range of [30 GHz-60 GHz] (mm-wave frequency range) with larger bandwidths. The values of f_i, f_{nyq}, and N are 40 GHz, 90 GHz, and 2, respectively. The sampling frequency for each channel is 90GHz/195. The reconstruction performance of MWC is successful for bandwidths of 100 MHz, 300 MHz, and 500 MHz.

Table 4
Performance of MWC for different bandwidths at millimeter-wave carrier frequency range

Bandwidth	Total Sampling rate	Number of channels	Reconstruction
100 MHz	13,846,153,847 Hz	30	Successful
300 MHz	13,846,153,847 Hz	30	Successful
500 MHz	13,846,153,847 Hz	30	Successful

4. Conclusion

The simulation results show that the MWC with 30 channels using a multichannel sub-Nyquist sampling method can successfully reconstruct multiband signals in 5G mobile networks. These channels and its sampling method reduce the total sampling rate and make the MWC capable of reconstructing multiband signals at a rate far below the Nyquist rate in 5G mobile communication networks in both frequency ranges. It shows that the system's performance can be affected negatively by bandwidth changes and the signal's carrier frequency. However, the results show that we can change the unsuccessful performance of the system to successful reconstruction by selecting the right carrier frequency for a Nyquist frequency. Moreover, findings indicate that in the sub-6 GHz frequency range, the reconstruction performance of the MWC can be more vulnerable to bandwidth changes compared to its performance in the frequency range from 30 GHz to 60 GHz.

References
[1] Shafi, Mansoor, Andreas F. Molisch, Peter J. Smith, Thomas Haustein, Peiying Zhu, Prasan De Silva, Fredrik Tufvesson, Anass Benjebbour, and Gerhard Wunder. "5G: A tutorial overview of standards, trials, challenges,

deployment, and practice." *IEEE journal on selected areas in communications* 35, no. 6 (2017): 1201-1221. https://doi.org/10.1109/JSAC.2017.2692307

[2] Gupta, Akhil, and Rakesh Kumar Jha. "A survey of 5G network: Architecture and emerging technologies." *IEEE access* 3 (2015): 1206-1232. https://doi.org/10.1109/ACCESS.2015.2461602

[3] Elkashlan, Maged, Trung Q. Duong, and Hsiao-Hwa Chen. "Millimeter-wave communications for 5G: fundamentals: Part I [Guest Editorial]." *IEEE Communications Magazine* 52, no. 9 (2014): 52-54. https://doi.org/10.1109/MCOM.2014.6894452

[4] Elkashlan, Maged, Trung Q. Duong, and Hsiao-hwa Chen. "Millimeter-wave communications for 5G–Part 2: applications [Guest Editorial]." *IEEE Communications Magazine* 53, no. 1 (2015): 166-167. https://doi.org/10.1109/MCOM.2015.7010530

[5] Daniels, Robert C., and Robert W. Heath. "60 GHz wireless communications: Emerging requirements and design recommendations." *IEEE Vehicular technology magazine* 2, no. 3 (2008): 41-50. https://doi.org/10.1109/MVT.2008.915320

[6] Foster, Brian, and Cormac Herley. "Exact reconstruction from periodic nonuniform samples." In *1995 International Conference on Acoustics, Speech, and Signal Processing*, vol. 2, pp. 1452-1455. IEEE, 1995. https://doi.org/10.1109/ICASSP.1995.480557

[7] Lin, Yuan-Pei, and P. P. Vaidyanathan. "Periodically nonuniform sampling of bandpass signals." *IEEE Transactions on Circuits and Systems Ii-Analog and Digital Signal Processing* 45, no. 3 (1998): 340-351. https://doi.org/10.1109/82.664240

[8] Kohlenberg, Arthur. "Exact interpolation of band-limited functions." *Journal of Applied Physics* 24, no. 12 (1953): 1432-1436.

[9] Maechler, Patrick, Norbert Felber, and Andreas Burg. "Random sampling ADC for sparse spectrum sensing." In *2011 19th European Signal Processing Conference*, pp. 1200-1204. IEEE, 2011.

[10] Donoho, David L. "Compressed sensing." *IEEE Transactions on information theory* 52, no. 4 (2006): 1289-1306.

[11] Laska, Jason N., Sami Kirolos, Marco F. Duarte, Tamer S. Ragheb, Richard G. Baraniuk, and Yehia Massoud. "Theory and implementation of an analog-to-information converter using random demodulation." In *2007 IEEE International Symposium on Circuits and Systems (ISCAS)*, pp. 1959-1962. IEEE, 2007. https://doi.org/10.1109/ISCAS.2007.378360

[12] Tropp, Joel A., Jason N. Laska, Marco F. Duarte, Justin K. Romberg, and Richard G. Baraniuk. "Beyond Nyquist: Efficient sampling of sparse bandlimited signals." *IEEE transactions on information theory* 56, no. 1 (2009): 520-544. https://doi.org/10.1109/TIT.2009.2034811

[13] Mishali, Moshe, and Yonina C. Eldar. "Sub-nyquist sampling." *IEEE Signal Processing Magazine* 28, no. 6 (2011): 98-124. https://doi.org/10.1109/MSP.2011.942308

[14] Mishali, Moshe, and Yonina C. Eldar. "Xampling: Analog data compression." In *2010 Data Compression Conference*, pp. 366-375. IEEE, 2010. https://doi.org/10.1109/DCC.2010.39

[15] Bronckers, Sander, Anne Roc'h, and Bart Smolders. "Wireless receiver architectures towards 5G: Where are we?." *IEEE Circuits and Systems Magazine* 17, no. 3 (2017): 6-16. https://doi.org/10.1109/MCAS.2017.2713306

[16] Sun, Hongjian, Wei-Yu Chiu, Jing Jiang, Arumugam Nallanathan, and H. Vincent Poor. "Wideband spectrum sensing with sub-Nyquist sampling in cognitive radios." *IEEE Transactions on Signal Processing* 60, no. 11 (2012): 6068-6073. https://doi.org/10.1109/TSP.2012.2212892

[17] Sun, Hongjian, Arumugam Nallanathan, Shuguang Cui, and Cheng-Xiang Wang. "Cooperative wideband spectrum sensing over fading channels." *IEEE Transactions on Vehicular Technology* 65, no. 3 (2015): 1382-1394. https://doi.org/10.1109/TSP.2012.2212892

[18] Sun, Hongjian, Arumugam Nallanathan, Cheng-Xiang Wang, and Yunfei Chen. "Wideband spectrum sensing for cognitive radio networks: a survey." *IEEE Wireless Communications* 20, no. 2 (2013): 74-81. https://doi.org/10.1109/MWC.2013.6507397

[19] Eldar, Yonina C. "Analog compressed sensing." In *2009 IEEE International Conference on Acoustics, Speech and Signal Processing*, pp. 2949-2952. IEEE, 2009. https://doi.org/10.1109/ICASSP.2009.4960242

[20] Mishali, Moshe, and Yonina C. Eldar. "From theory to practice: Sub-Nyquist sampling of sparse wideband analog signals." *IEEE Journal of selected topics in signal processing* 4, no. 2 (2010): 375-391. https://doi.org/10.1109/JSTSP.2010.2042414

[21] Mishali, Moshe, and Yonina C. Eldar. "Reduce and boost: Recovering arbitrary sets of jointly sparse vectors." *IEEE Transactions on Signal Processing* 56, no. 10 (2008): 4692-4702. https://doi.org/10.1109/TSP.2008.927802

[22] Saifulizam, Minhah Mardhiyyah, Ismahafezi Ismail, Wan Mohd Amir Fazamin Wan Hamzah, Maizan Mat Amin, and Hoshang Kolivand. "A Systematic Literature Review: User Experience in Virtual Reality Prototyping." *Journal of Advanced Research Design* 123, no. 1 (2024): 91-107. https://doi.org/10.37934/sijese.3.1.1527

[23] Sivakumar, Renukka, Saidatul Norlyana Azemi, Yeng Seng Lee, Yeow You Kok, and Jack Soh Ping. 2024. "3-D Printed Antennas with Dielectric Lens for Free-Space Constitutive Parameters Measurement". *Semarak International Journal of Electronic System Engineering* 1, no. 1 (2024): 1-25. https://doi.org/10.37934/sijese.1.1.125

[24] Tan Ling Choon, Danny, Azura Hamzah, Ahmad Haziq Aiman Rosol, and Mahroof Mohamed Mafroos. "Optimizing The Pump Power and Frequencies of Raman Amplifiers for Gain Flatness". *Semarak International Journal of Electronic System Engineering* 3, no. 1 (2024): 46-55. https://doi.org/10.37934/sijese.3.1.4655